Applied Physics Letters PERSPECTIVE scitation.org/journal/apl

Opportunities for energy level tuning at inorganic/organic semiconductor interfaces

Cite as: Appl. Phys. Lett. **119**, 260501 (2021); doi: 10.1063/5.0074963
Submitted: 12 October 2021 · Accepted: 16 November 2021 ·
Published Online: 27 December 2021

Norbert Koch[a)]

AFFILIATIONS

Institut für Physik and IRIS Adlershof, Humboldt-Universität zu Berlin, Berlin, Germany and Helmholtz-Zentrum Berlin für Materialien und Energie GmbH, Berlin, Germany

[a)]Author to whom correspondence should be addressed: norbert.koch@physik.hu-berlin.de

ABSTRACT

The aim of this Perspective is to provide an overview of approaches that can be employed to tune the energy level alignment at interfaces between inorganic and organic semiconductors for use in electronic and optoelectronic devices. The approaches include tailoring intramolecular dipolar bond distribution, controlling molecular orientation at interfaces, and the insertion of a molecularly thin interlayer that abruptly shifts the electrostatic potential between the two semiconductors and, thus, affords level tuning. With these state of the art methods, the frontier energy levels at an inorganic/organic heterojunction can be varied up to ca. 3 eV, i.e., covering the energy gap of most semiconductors. By combining two or more of these approaches or by employing interfacial molecular switches, it is envisioned that unconventional and dynamically switchable interfacial energy level scenarios can be created, enabling expanded or superior device functionality.

I. INTRODUCTION

Semiconductor heterojunctions are key enablers for advanced electronic and optoelectronic devices. The relative position of the frontier electronic energy levels at a junction determines its functionality with respect to the fundamental interfacial energy and charge transfer processes.[1] For instance, a straddling type-I level alignment supports excited state energy transfer from one to the other component, whereas a junction with staggered type-II energy levels facilitates charge separation of an excited state close to the interface. By deliberately adjusting the energy level offset at the heterojunction, the flow of energy and charges can be directed. Consequently, huge efforts have been and still are dedicated to achieve control over the energy levels at interfaces.[2,3] For inorganic semiconductors, this is particularly challenging because the formation of covalent bonds at the interface between two dissimilar materials can result in adverse gap states, and crystal lattice mismatch can induce strain and hamper appropriate structure formation. Realizing atomically sharp inorganic heterojunctions remains challenging. One ansatz to circumvent this problem is the deposition of a van der Waals semiconductor onto the surface of a conventional inorganic semiconductor, i.e., covalent bond formation across the interface does not occur and the two materials largely retain their individual properties. Layered inorganic two-dimensional (2D) materials, such as transition metal dichalcogenides, have significant potential in this respect.[4] However, their electronic properties strongly depend on the number of layers, as well as on strain that may be introduced during layer transfer, and energy level tuning for a given material pair has not yet been explored. Instead, this Perspective focuses on organic materials as alternative van der Waals semiconductors for combination with inorganic ones, as several energy level tuning approaches have emerged that hold potential for wider use in devices. Most organic semiconductors—molecules or polymer-based—feature strong light–matter coupling, making them particularly attractive for optoelectronic applications.[5] However, it is difficult to obtain highest charge carrier mobilities in organic semiconductors. Therefore, their combination with established inorganic semiconductors, which can exhibit record-high carrier mobility, provides the potential for the combination of the best of the two worlds in inorganic–organic heterojunctions. In the following, first a few peculiarities of inorganic and organic semiconductors with respect to their electronic properties are briefly revisited to enhance perception of those with a background in only one of the two material classes. Then different approaches to tune the energy level alignment at their heterojunctions are explained, alongside a few specific examples, and then ending with an outlook on how the field could further evolve.

II. RECALLING BASIC ELECTRONIC PROPERTIES OF ISC–OSC INTERFACES

As noted above, the relative position of the two components' frontier electronic energy levels is decisive for the junction's functionality. These are the valence band maximum (VBM) and conduction band minimum (CBM) of the inorganic semiconductor (iSC), and the highest occupied molecular orbital (HOMO) level and lowest unoccupied molecular orbital (LUMO) level of the organic semiconductor (oSC). Strictly, HOMO and LUMO levels pertain to molecular semiconductors without long-range order, and in thin films disorder-induced energy level fluctuations lead to an energy-distribution of the levels often approximated by a Gaussian distribution. For crystalline molecular semiconductors, overlap between HOMOs and LUMOs of neighboring molecules can result in electron delocalization and in the formation of dispersive bands (i.e., the energy of electronic states varies with momentum)[6] but typically with narrower width compared to iSCs. Many polymeric oSCs also feature dispersive electronic bands along the polymer chain,[7] so that the terms VBM and CBM are more appropriate than the use of HOMO and LUMO; the reader should yet be aware that both sets of terminology are often used interchangeably in the literature. Note, electronic band dispersion is different from energetic dispersion of comparably localized states, as sometimes used in the literature to denominate energetic disorder.[8] The energy required to remove an electron from the VBM or HOMO level to infinite distance is the ionization energy (IE), and the energy gained upon adding an electron from infinity to the CBM or LUMO level is the electron affinity (EA). In practical terms and for solids, the IE and EA are given with respect to the vacuum level, i.e., the zero of the electrostatic potential (E_0) above the sample surface as depicted in Fig. 1(a). This figure also shows how the interfacial energy level alignment is often estimated and sketched in the literature, i.e., the respective IE and EA values—most frequently determined by ultraviolet photoelectron and inverse photoelectron spectroscopies (UPS and IPES)[9,10] for the individual materials—are plotted next to each other assuming a constant electrostatic potential within the materials and across the interface, indicated by a constant E_0. This simple representation, however, falls short of taking into account even the most basic phenomena that occur at such interfaces.

First, most surfaces of iSCs exhibit a significant surface density of states (sDOS) due to surface reconstruction compared to the bulk atomic structure, and depending on preparation conditions also foreign atoms may be included to saturate dangling bonds.[2,11] Often the sDOS lies in energy within the otherwise empty gap of the semiconductors as illustrated in Fig. 1(b) for donor type surface states close to the CBM. The Fermi level (E_F) is then pinned within the sDOS, closer to the CBM than in the bulk far from the surface. Accordingly, an electron accumulation region close to the surface forms and induces surface band bending (SBB) to establish electronic equilibrium throughout the semiconductor. The direction and magnitude of the SBB, which is an electrostatic phenomenon that shifts all energy levels including E_0 in parallel, depends on the doping type and level of the iSC, the position and density of the surface states, as well as the material's dielectric constant[2,12] and can amount to several hundred meV. This also implies that the iSC work function (Φ), being a surface property of a sample, is not a constant material parameter. It is noted that Φ of a semiconductor, defined as the energy difference between E_F at the sample surface and E_0 just outside the sample,[1,13] depends strongly

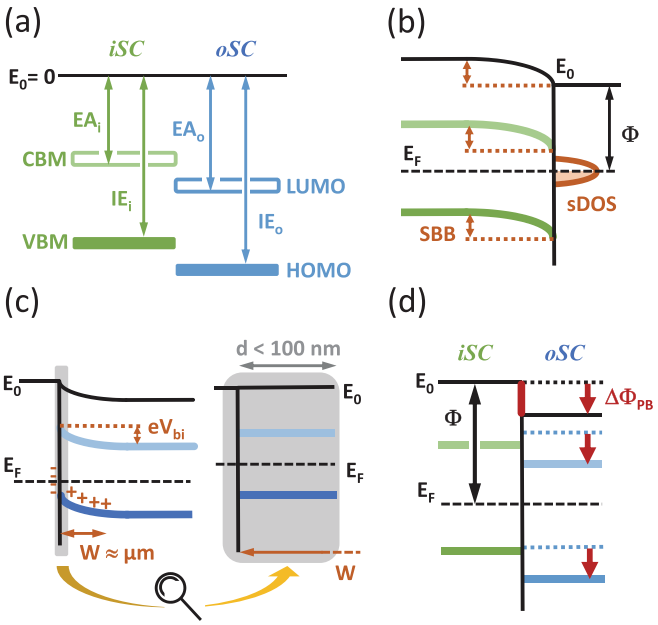

FIG. 1. (a) Schematic of how the energy level alignment at iSC/oSC interfaces is frequently estimated by assuming a constant electrostatic potential zero (E_0) across the interface, and using separately determined values for the ionization energy (IE) and electron affinity (EA) (with subscripts "i" and "o" to represent the inorganic and organic materials, respectively). (b) An iSC surface with a finite surface density of states (sDOS) that induces surface band bending (SBB). (c) Left part: energy levels within an undoped oSC away from a generic interface with ground state charge transfer, leading to energy level bending that is characterized by the built-in field (V_{bi}) and depletion layer width (W). Right part: zoom into the near-interface region when the oSC film thickness is much smaller than W, giving the appearance of flat energy levels away from the interface. (d) Illustration of the electronic "push back" effect at an iSC/oSC van der Waals type interface, where the deposition of the oSC lowers E_0 and, thus, the work function of the iSC by $\Delta\Phi_{PB}$, altering the level alignment compared to an estimation with constant E_0.

on the semiconductor doping level and the sDOS distribution. If the surface reconstruction involves polar bonds with components of their dipole moment in the direction of the surface normal, an additional surface dipole will modify Φ, and in consequence also IE and EA are sample-dependent parameters rather than material constants.

In contrast, oSCs are characterized by a closed-shell electronic configuration, so that molecules or polymer chains at the surface of a solid feature the same electronic structure as in the bulk. Therefore, a significant sDOS within the energy gap is not an issue, and notable SBB has not been reported. However, oSCs can feature gap states in the bulk, which are mostly due to structural disorder in thin films.[14,15] Furthermore, modern oSC materials are highly purified and exhibit very low (unintentional) doping levels. This explains why the energy levels of oSCs appear "flat" as a function of distance from almost any interface in contrast to the expectation that interfacial charge transfer and associated band bending (often termed built-in field, eV_{bi}) should occur if Φ of the second interface component (regardless of whether this is a conductor or semiconductor) is different from that of the oSC [see Fig. 1(c)]. The underlying reason is of practical nature: the low intrinsic carrier concentration of pure oSCs results in a comparably

large width (W) of the interfacial charge accumulation or depletion region,[2] extending up to several μm. In devices, the typical layer thickness of oSCs is on the order of 100 nm or less, and thus only this thickness range is typically studied in experiments. When one then zooms into the near-interface region [grey shaded area in Fig. 1(c)], the layer thickness is significantly smaller than W, and thus, the energy levels seem to be flat. This was nicely demonstrated in experiment by Ishii *et al.*[16] When the oSC is intentionally doped, interfacial band bending is clearly observed[17,18] and must, therefore, also be considered in energy level diagrams.

Third, Φ of the bare iSC surface can be reduced by adsorption of an oSC by the "push-back effect." It has been recognized early on for metal surfaces that its Φ has a contribution from a surface dipole,[19] because electrons at the surface "spill out" into the free space compared to the positively charged nuclei. Any adsorbates, also van der Waals bonded ones, push this electron density back toward the bulk due to Pauli repulsion, thereby reducing the surface dipole magnitude and, thus, Φ.[20,21] The reduction of Φ by this effect ($\Delta\Phi_{PB}$) can be on the order of 1 eV for metals due to their high free carrier density. For iSCs, this push-back effect also occurs, but it is typically smaller in magnitude due to a lower free carrier density; yet, a few 100 meV have been reported.[22,23] If not properly accounted for, $\Delta\Phi_{PB}$ can lead to quantitative and even qualitative improper approximation of the interfacial energy level alignment as shown in Fig. 1(d).

The consequence of these basic interfacial phenomena is that the estimation of the energy level alignment between iSCs and oSCs can be significantly flawed due to oversimplifications. It is, therefore, highly recommended to experimentally determine the actual level alignment and to identify the underlying mechanisms, as otherwise correlation with device function and performance can be misleading for subsequent development and improvement.

III. ENERGY LEVEL TUNING VIA MATERIAL DESIGN

It is obvious that the energy level alignment can be changed by choice of materials both inorganic and organic. Particularly oSCs feature the advantage that their energy gap, IE, and EA can be varied over a wide range by adapting the molecular structure. However, for both types of materials, composition and structural changes may result in inferior electronic and optoelectronic properties, so that one could face the situation of aiming to adjust the energy levels for one particular iSC–oSC material pair. In this case, the often pronounced structural anisotropy of oSCs, e.g., resembling rods or plates, the intramolecular polar bonds, and the intermolecular packing (crystal structure) may be taken advantage of. For ordered molecular assemblies, IE and EA are strongly dependent on the molecular orientation with respect to a surface or interface.[24] The underlying reason is that collective electrostatic effects, arising from the overall charge density distribution within molecules and their neighbors, modify E_0 with respect to the electronic levels. For instance, one benzene ring features higher electron density in the delocalized π-orbitals above and below the plane formed by the carbon nuclei, whereas the peripheral C–H bonds are polar with a higher positive charge density at the hydrogens. In a hypothetical macroscopic ordered assembly of benzene molecules in a simple cubic structure with coplanar molecular planes, E_0 outside the assembly is higher above the molecular electronic levels in the direction perpendicular to the molecular planes, and vice versa in the direction along the planes. This can be viewed as an analogon to the surface dipole of metals, but here two opposite directions of the surface dipole are possible, just depending on the charge density pattern determined by the molecular structure and their packing. In turn, IE and EA are larger in the direction perpendicular to the benzene planes compared to the direction along the planes, i.e., IE and EA depend on the orientation of the molecules with respect to a surface or interface. For many prototypical oSCs, intramolecular dipoles and quadrupoles are the leading terms that contribute to the orientation-dependent IE and EA.[24–26] Note, the energy gap of the molecules is, of course, not affected, as all energy levels of the molecules are only rigidly shifted with respect to E_0.[27] If one succeeds in controlling the orientation of molecules with respect to an iSC surface, it is then possible to adjust the interfacial energy level alignment as sketched in Fig. 2, where rod-like or plate-like molecules are either lying flat on the iSC (left) or upright standing (right). The difference in IE and EA between such two orientations is on the order of 0.5–1 eV already for simple oSCs, such as pentacene and phenylene- or thienylene-oliogmers, and thus, huge changes of the energy level alignment can be implemented.[28] The example of Fig. 2 shows that the oSC with lying molecules would act as interfacial electron acceptor, whereas the *same* oSC with standing molecules would act as electron donor.

Controlling the molecular orientation with respect to an interface is certainly a challenge.[29] One possible means is a modification of the iSC surface energy. The associated change of the surface composition, however, can result in a modified Φ and also unwanted surface states. Alternatively, the growth conditions of the oSC can be adapted with the aim of kinetically trapping one of the two molecular orientations. Yet, one can face the situation that the first molecular layer is lying on the iSC surface, but already the second layer and multilayers grow upright standing, thus ending up with a rather complex interfacial energy landscape.[23] Both aforementioned approaches require substantial experimental efforts. A more practical method is making comparably subtle changes to the molecular structure. Most oSCs feature peripheral C–H bonds, i.e., local dipoles with the positive end on the hydrogen. Substitution of hydrogen for fluorine reverses the direction of the peripheral dipoles with only moderate effects on the energy gap of the molecule. Such a change in intramolecular charge density distribution, presumed that intermolecular packing is not strongly affected,

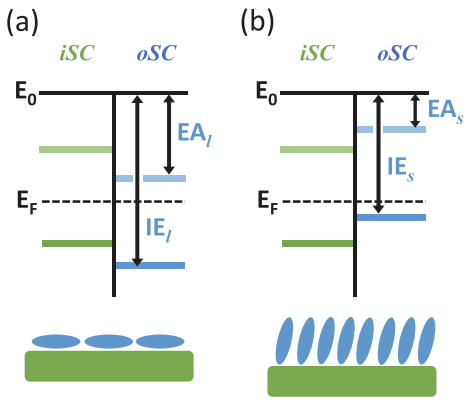

FIG. 2. Illustration of how the orientation-dependent ionization energy (IE) and electron affinity (EA) of oSCs can impact the interfacial energy level alignment, subscript *l* for lying molecules in (a) and subscript *s* for standing molecules in (b).

then reverses the trends (shown in Fig. 2) of IE and EA between lying and standing molecules at the interface with the iSC, i.e., lying molecules would feature lower IE and EA compared to standing ones. Admittedly, while controlling the molecular orientation at an interface allows remarkable tuning the energy level alignment by over one 1 eV, this approach can turn out to be tedious in practice. The strategies discussed next, i.e., employing an ultrathin molecular interlayer (IL) between iSC and oSC to affect the interfacial electrostatic potential, are likely more practicable.

IV. ULTRATHIN MOLECULAR INTERLAYERS BETWEEN ISC AND OSC

The conceptual foundation of using a molecularly thin interlayer between an iSC and an oSC to tune the interfacial energy level alignment is the fact that a two-dimensional (2D) dense array of electric dipoles, oriented perpendicular to the 2D plane, leads to an abrupt change of the electrostatic potential between one and the other side of that plane.[30] Therefore, an adequately designed dipolar interlayer is capable of shifting the energy levels of iSC and oSC with respect to each other. To minimize adverse effects of the interlayer on interfacial charge and energy transfer processes, the dipolar layer should be as thin as possible and should not possess energy levels in the energy gaps of the two involved semiconductors. Two approaches that mostly fulfill these requirements are the use of (i) a self-assembled monolayer (SAM) of dipolar molecules and (ii) a monolayer of strong molecular electron donors or acceptors that undergo ground state charge transfer with the iSC. In either of the two approaches, the interlayer is first deposited onto the iSC surface, leading to an increased or decreased work function by $\Delta\Phi$ compared to the bare surface Φ. This, in turn, results in a modified position of the subsequently deposited oSC's HOMO and LUMO levels with respect to the VBM and CBM of the iSC, as schematically depicted in Fig. 3. The magnitude of $\Delta\Phi$ change can be retrieved from the Helmholtz equation

$$\Delta\Phi = \frac{qN\mu_{\perp}}{\varepsilon_0\varepsilon_{eff}}.$$

Here, q is the elementary charge, N is the area density of dipoles, $\mu_{\perp}$ is the dipole moment perpendicular to the 2D plane, ε_0 is the vacuum permittivity, and ε_{eff} is the effective dielectric constant within the 2D plane of dipoles.[30] The magnitude of ε_{eff} for dipolar molecules in a SAM has been calculated to amount up to 3 for commonly used dipolar moieties,[31] and that of molecular donor/acceptor monolayers on an iSC have not yet been investigated in detail.

Particularly attractive for the formation of dipolar SAM interlayers are molecules that can bind covalently to the surface of the iSC in solution-based processes, as this warrants uniaxial alignment of the dipoles, can help to reduce the iSC sDOS by saturating dangling bonds,[32] and is a cost-effective method compatible with solution-processing of many oSCs. A range of functional groups for that purpose has been introduced such as silanes, thiols, and many more.[33] The direction and magnitude of the molecules' dipole moment can be adjusted over wide ranges by adequate substitution. Note that the covalent bond to the iSC brings about a further contribution to $\Delta\Phi$ in addition to that given by the Helmholtz equation above, and this bond-dipole is specific for the employed iSC and bonding-motif.[30] Among the possible binding-groups, phosphonic acid derivatives have found widest applications, because phosphorous in the phosphonate

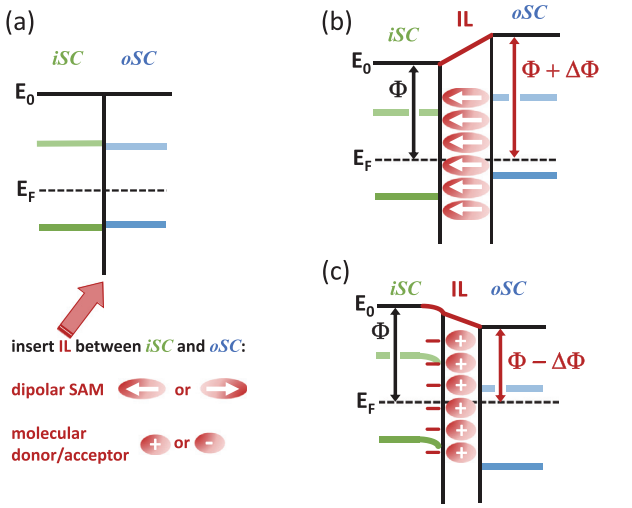

FIG. 3. Schematic of (a) how the insertion of a molecular interlayer (IL) can result in a modified interfacial energy level alignment based on the IL-induced change of the iSC work function ($\Delta\Phi$), (b) by a self-assembled monolayer (SAM) of dipolar molecules (per convention, the dipole moment direction points from the negative to the positive charge of the dipole), and (c) a molecular electron donor layer that undergoes ground state charge transfer with the iSC.

head groups engages predominantly in bi-dentate or tri-dentate interactions with virtually any metal oxide surfaces[34–36] or natively oxidized semiconductor surfaces.[37] The two or even three covalent bonds to the surface per molecule result in superior mechanical robustness of the interface, while the footprint area of the head group still allows for close-packing of the molecules in a SAM.[37] As an example, the work function of ZnO was varied between 4.1 and 5.6 eV by using different phosphonic acid derivatives for SAM formation.[38] This led to huge changes in the energy level alignment with different oSCs, spanning the ability of the modified ZnO to either inject electrons or holes into the oSC.

Fine-tuning of $\Delta\Phi$ with one type of dipolar molecules is difficult, because the SAM packing is usually dense and can be barely controlled. However, by using two types of molecules with different dipole moment and good miscibility in SAMs, it is possible to fine-tune $\Delta\Phi$ in the interval given by the two individual SAMs by the mixing ratio of the two molecules in the SAM. This was evidenced for two different phosphonic acid derivatives and ZnO, and the energy level offset between the iSC and the oSC *N*,*N*′-di(1-naphthyl)-*N*,*N*′-diphenyl-(1,1′-biphenyl)-4,4′-diamine (α-NPD) could also be tuned according to the achieved $\Delta\Phi$.[39] Quite notably, despite the fact that the dipolar SAM was introduced between iSC and oSC, interfacial charge transfer absorption and emission were found for the ZnO/interlayer/α-NPD, whose energy followed the SAM-tuned energy level alignment. The origin of this absorption and emission are radiative transitions between an electron in ZnO and a hole in α-NPD, implying that there is sufficient wave function overlap between the states in the two semiconductors despite the ca. 1 nm spatial separation by the SAM.

Compared to dipolar SAMs, an even wider range of $\Delta\Phi$—and thus, level alignment tuning—can be realized by depositing a monolayer of a strong electron donor or acceptor molecule on the surface of the iSC before depositing the oSC. As shown in Fig. 3(c) for the

example of an interlayer of molecular donors, the ground state charge transfer between iSC and the donor molecules also induces a $\Delta\Phi$. This phenomenon was first introduced for changing Φ of diamond,[40] metal,[41] and graphene[42] surfaces. The modified Φ of the iSC surface then re-aligns the energy levels of the oSC accordingly. The source of charges transferred from the iSC to the molecular interlayer can, of course, be the states at the VBM/CBM, but the IE/EA values of many iSCs are not within the range for practicable EA/IE values of corresponding acceptor/donor molecules. In practice, for most iSCs charge reservoirs for this interfacial charge transfer are donor/acceptor type levels in the bulk (energy levels of bulk dopants), tail states extending into the bandgap from the VBM/CBM and the sDOS. Consequently, the total work function change induced by the molecular interlayer has two contributions, i.e., $\Delta\Phi = \Delta\Phi_{BB} + \Delta\Phi_{ID}$, where $\Delta\Phi_{BB}$ is due to band bending induced at the iSC surface (or a change of the SBB of the bare surface) and $\Delta\Phi_{ID}$ due to the dipoles generated by the charged molecules and the counter-charges at the iSC surface. A detailed account of the two contributions is given in Refs. 43 and 44, and it should suffice to highlight in this Perspective the important role of the iSC's doping level and sDOS on the relative contribution of $\Delta\Phi_{BB}$ and $\Delta\Phi_{ID}$ to $\Delta\Phi$. For low doping levels, $\Delta\Phi_{BB}$ is the dominant contribution, and $\Delta\Phi_{ID}$ becomes the prevailing term only close to degenerate doping levels. When the sDOS becomes larger, the contribution of $\Delta\Phi_{BB}$ to the overall work function change becomes smaller. Another important correlation is that the amount of charge transferred to the molecular interlayer decreases significantly when lowering the doping level of the iSC. For instance, the work function of moderately doped ZnO was increased by 2.8 eV by depositing a monolayer of the molecular acceptor tetrafluoro-tetracyanoquinodimethane (F4TCNQ), but the amount of charge transfer was found to be only 0.02 electrons per molecule, or, when considering that time-averaged a molecule can only accept an integer charge, only one out of 50 molecules in the monolayer carries an electron.[45] Due to this low density of charged molecules, direct evidence for integer charges in a molecular acceptor interlayer was presented only recently.[46]

For a number of iSCs (predominantly Si, GaN, and ZnO) and strong molecular donors and acceptors, a remarkably wide range of Φ-tuning was reported, approximately covering the range from 2.3 eV (Refs. 47 and 48) to 6.0 eV.[43,45] This range is wider than the energy gap of most oSCs, so that—in principle—it should be possible to tune the iSC/oSC energy level alignment for a given material pair over the entire range of the oSC energy gap. Actually, for Si and two prototypical organic semiconductors, this tunability was demonstrated experimentally within the limits of the *intrinsic* Fermi level pining at the HOMO/LUMO level manifolds of the oSCs.[49] Conventionally, the term "Fermi level pinning" is used to denote a situation where E_F is pinned at gap states of the semiconductor.[1] Here, the term "intrinsic Fermi level pinning" should emphasize that E_F becomes pinned at the frontier energy levels of the semiconductor, i.e., in the absence of gap states. It is also worth pointing out that one of the oSCs employed was deposited from solution, showing that the interlayer approach with molecular donors/acceptors is compatible with cost-efficient and large-area deposition methods.

Examples for non-trivial interfacial energy level tuning are shown in Figs. 4(a) and 4(b). Figure 4(a) depicts the interlayer-tuned energy level alignment achieved for the interface of n-doped ZnO and a blue luminescent organic semiconductor from the ladder-type

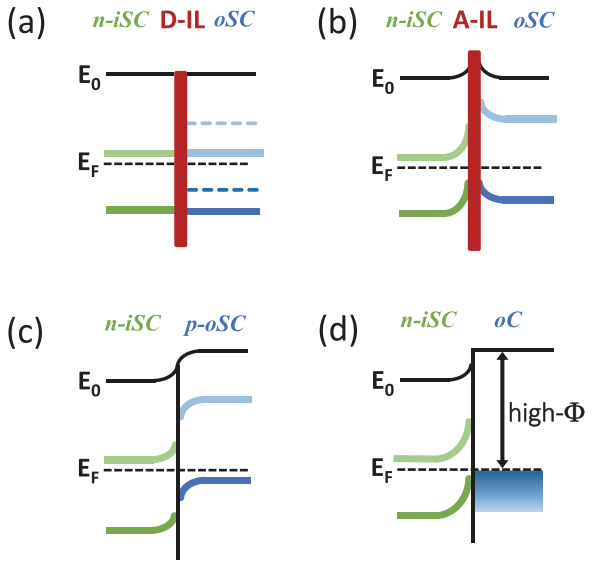

FIG. 4. Examples of non-trivial interfacial energy level scenarios discussed in the text. (a) n-doped iSC and intrinsic oSC, where the level alignment was changed by a molecular donor interlayer (D-IL) compared to without D-IL. (Dashed lines on the oSC side indicate the energy levels *without* D-IL.) (b) Upward band bending on both sides of the heterojunction due to a molecular acceptor interlayer (A-IL), leading to surface band bending in the iSC and intrinsic Fermi level pinning induced energy level bending within the oSC. (c) "Classical" *pn*-junction formed at the interface between an n-doped iSC and a p-doped oSC. (d) Near-interface inversion layer formation in an n-doped iSC by the deposition of a high work function organic conductor (oC).

oligophenylene class, whose energy gap was matched to that of ZnO. The intrinsic energy level alignment between the two materials was of staggered type-II [dashed lines in Fig. 4(a)] with an energy offset between the CBM/LUMO and VBM/HOMO of over 1 eV. Optical excitation of ZnO resulted in efficient energy transfer to the organic material because of matched emission (ZnO) and absorption (oSC) spectra. However, excitons formed in the oSC by the energy transfer readily experienced interfacial charge transfer (electron transfer to ZnO, the hole remaining in the oSC) because of the large energy level offset. Consequently, luminescence from the organic light emitter was very weak. In contrast, with an interlayer of the strong electron donor ruthenium pentamethylcyclopentadienyl mesitylene, the energy offset between the iSC and oSC levels was brought to less than 0.1 eV (in essence type-I), and the luminescence from the organic semiconductor increased by a factor of seven.[47]

Figure 4(b) shows the interlayer-tuned level alignment between n-doped Si and α-NPD. The pristine iSC/oSC interface, i.e., without interlayer, exhibited a straddling type-I level alignment (not shown) with 0.3 eV upward surface band bending within Si due to surface states and flat energy levels within the undoped oSC. The deposition of the molecular acceptor hexafluoro-tetracyanonaphthoquinodimethane (F6TCNNQ) as interlayer onto Si increased Φ significantly to 5.3 eV, as expected according to the description of Fig. 3. Part of this Φ-increase was due to interlayer-enhanced upward surface band bending within Si, now amounting to 0.6 eV. This high Φ of the Si surface was sufficient to induce *intrinsic* Fermi level pinning at the HOMO manifold of α-NPD,

because the IE of α-NPD matched the modified Si work function. The intrinsic Fermi level pinning at the HOMO manifold induced positive space charge in α-NPD close to the interface, resulting in concomitant upward energy level bending within the oSC [see Fig. 4(b)], instead of the flat levels away from the interface obtained without the molecular interlayer. The result is a rather unusual energy level situation, where both semiconductors exhibit upward band bending toward their interface and holes in both materials are confined right to the interface [cf. Fig. 4(b)].[49] The electrical characteristics of such an interface remain yet to be investigated.

Figure 4(c) depicts the energy level alignment achievable when both semiconductors are doped, and classical *pn*-junctions can be formed, as the depletion width within the oSC becomes smaller (a few 10 nm or less) for higher doping levels. Yet, evaluation of the depletion width must be done carefully as diffusion and preferred adsorption of molecular dopants used for oSCs (often the same donor/acceptor molecules used for interlayers, see above) can induce additional Φ changes. Notable for the organic electronics community, the determination of the depletion width within the oSC can be used as a complementary experimental method to assess the doping efficiency.[50]

The final example, shown in Fig. 4(d), does not strictly pertain to an oSC, but rather to an organic conductor, often used as an electrical contact in organic electronic devices. These are often realized by degenerately doping a polymer semiconductor, the most widespread and commercially available one being poly(3,4-ethylenedioxythiophene) that is *p*-type doped by polystyrene sulfonate (PEDOT:PSS). Numerous different formulations have been introduced, and—depending on application—they feature moderate to high electrical conductivity and/or high work functions, well in excess of 5 eV, which enables Ohmic hole injection at contacts to undoped oSCs. When such a high-Φ conductor is brought into contact with an n-doped iSC that typically would have comparably low Φ, electrons flow from the iSC to the organic conductor to establish electronic equilibrium at the interface. The resulting electron deficiency in the iSC close to the interface leads to a depletion region with associated upward band bending. For n-doped Si, it was demonstrated that PEDOT:PSS deposition even resulted in the formation of an inversion layer near the surface,[51] i.e., while E_F is close to the CBM in the bulk, it is very close to the VBM at the surface [cf. Fig. 4(d)]. Above-bandgap light absorbed by Si produces free charge carriers, and this particular energy level situation then facilitates efficient hole collection by the PEDOT:PSS contact while electrons are collected at the back-contact of Si (not shown). This structure can be viewed as a thin *pn*-junction within Si and, thus, a solar cell, where the p-doped region in Si does not have to be formed by elaborate classical doping; instead it forms spontaneously upon polymer deposition.[52] Model solar cells based on iSC/conductive polymers have achieved over 13% power conversion efficiency to date.[53,54] One further beneficial effect of the conductive polymer has been suggested to be improved passivation of electronically active defects of the Si surface,[55] which could also be enhanced by the admixture of sorbitol to the PEDOT:PSS dispersion.[56] Because of the significant potential of this approach to reduce costs of solar cell fabrication, such interfaces between iSCs and conductive organic materials are presently the topic of investigation.[53,54,57]

V. OUTLOOK

There are a number of approaches that enable wide tuning of the energy level alignment at iSC/oSC interfaces, as collated above. For a given material pair, there will probably be more complexity than illustrated here, because the effects summarized in Fig. 1 have not been fully accounted for in the discussion of the individual approaches, for brevity. For real interfaces, one should carefully analyze the phenomena that factually occur and the ones that dominate the achieved energy level alignment. Particularly surface states of iSCs, which are highly sample-dependent, must be carefully considered. Suggesting general rules would, therefore, not be practical. Nonetheless, the basis for energy level adjustment is understood, and it will be interesting to see their use in a wider range of structures and devices in the future. One example could be the control of charge carrier density at an iSC surface by massive charge transfer to an organic interlayer, thereby generating or manipulating the properties of a two-dimensional electron (hole) gas confined to the hybrid junction. The formation of an *np*-inversion layer in an iSC with a high-Φ conductive polymer has been demonstrated. What is currently missing are corresponding low-Φ conductive polymers, ideally lower than the ca. 3.5 eV achieved with thin insulating polyethylenimine layers,[58] that would enable the formation *pn*-inversion layer, and thus providing more flexibility for device fabrication. Furthermore, all of the above methods allow static energy level tuning only, i.e., the energy levels are fixed once the junction is formed. For multifunctional devices, e.g., where more than one external stimulus can be used to control the device output, the use of photochromic molecules has already been shown to be highly attractive.[59–62] For instance, the energy gap of photochromic molecules can be switched between two values by selective light irradiation, and it was demonstrated that the output of organic field effect transistors[59,60] as well as organic light emitting diodes[61–63] can then be manipulated electrically and optically. These molecules can readily be functionalized with a phosphonic acid group so that defined formation of a dense and covalently bound SAM on an iSC surface is feasible.[64] It yet remains to be tested to what extent the function of an inorganic/organic semiconductor junction can be expanded by the insertion of such a photo-addressable interlayer. By combining two or even more of the named approaches, innovative energy level alignment situations at iSC/oSC interfaces can be envisioned, conceivably leading to superior electronic and optoelectronic functionality.

ACKNOWLEDGMENTS

The author is grateful for funding by the Deutsche Forschungsgemeinschaft (DFG, German Research Foundation) via Project No. 182087777-SFB 951.

AUTHOR DECLARATIONS

Conflict of Interest

The author has no conflict of interest to declare.

DATA AVAILABILITY

Data sharing is not applicable to this article as no new data were created or analyzed in this study.

REFERENCES

[1]S. M. Sze and K. K. Ng, *Physics of Semiconductor Devices* (John Wiley & Sons, Inc., Hoboken, NJ, 2006).
[2]W. Mönch, *Semiconductor Surfaces and Interfaces* (Springer, Berlin/Heidelberg, 1995).

[3]M. Fahlman, S. Fabiano, V. Gueskine, D. Simon, M. Berggren, and X. Crispin, Nat. Rev. Mater. **4**, 627 (2019).
[4]Y. Liu, N. O. Weiss, X. Duan, H.-C. Cheng, Y. Huang, and X. Duan, Nat. Rev. Mater. **1**, 16042 (2016).
[5]A. Köhler and H. Bässler, *Electronic Processes in Organic Semiconductors* (Wiley-VCH Verlag GmbH & Co. KGaA, Weinheim, Germany, 2015).
[6]Y. Nakayama, S. Kera, and N. Ueno, J. Mater. Chem. C **8**, 9090 (2020).
[7]M. Lögdlund and W. R. Salaneck, *Semiconducting Polymers* (Wiley, 1999), pp. 115–148.
[8]D. Venkateshvaran, M. Nikolka, A. Sadhanala, V. Lemaur, M. Zelazny, M. Kepa, M. Hurhangee, A. J. Kronemeijer, V. Pecunia, I. Nasrallah, I. Romanov, K. Broch, I. McCulloch, D. Emin, Y. Olivier, J. Cornil, D. Beljonne, and H. Sirringhaus, Nature **515**, 384 (2014).
[9]S. Hüfner, *Photoelectron Spectroscopy* (Springer, Berlin/Heidelberg, 2003).
[10]A. Kahn, Mater. Horiz. **3**, 7–10 (2016).
[11]P. Laukkanen, M. P. J. Punkkinen, M. Kuzmin, K. Kokko, J. Lång, and R. M. Wallace, Appl. Phys. Rev. **8**, 011309 (2021).
[12]L. Kronik and Y. Shapira, Surf. Sci. Rep. **37**, 1–206 (1999).
[13]J. Bardeen, Phys. Rev. **71**, 717 (1947).
[14]J. H. Kang, D. da Silva Filho, J.-L. Bredas, and X.-Y. Zhu, Appl. Phys. Lett. **86**, 152115 (2005).
[15]J. P. Yang, F. Bussolotti, S. Kera, and N. Ueno, J. Phys. D **50**, 423002 (2017).
[16]H. Ishii, N. Hayashi, E. Ito, Y. Washizu, K. Sugi, Y. Kimura, M. Niwano, Y. Ouchi, and K. Seki, Phys. Status Solidi **201**, 1075 (2004).
[17]W. Gao and A. Kahn, Appl. Phys. Lett. **79**, 4040 (2001).
[18]S. Olthof, W. Tress, R. Meerheim, B. Lüssem, and K. Leo, J. Appl. Phys. **106**, 103711 (2009).
[19]R. Smoluchowski, Phys. Rev. **60**, 661 (1941).
[20]H. Ishii, K. Sugiyama, E. Ito, and K. Seki, Adv. Mater. **11**, 605 (1999).
[21]G. Witte, S. Lukas, P. S. Bagus, and C. Wöll, Appl. Phys. Lett. **87**, 263502 (2005).
[22]S. Winkler, J. Frisch, R. Schlesinger, M. Oehzelt, R. Rieger, J. Räder, J. P. Rabe, K. Müllen, and N. Koch, J. Phys. Chem. C **117**, 22285 (2013).
[23]R. Schlesinger, S. Winkler, M. Brandt, S. Blumstengel, R. Ovsyannikov, A. Vollmer, and N. Koch, Phys. Chem. Chem. Phys. **21**, 15072 (2019).
[24]S. Duhm, G. Heimel, I. Salzmann, H. Glowatzki, R. L. Johnson, A. Vollmer, J. P. Rabe, and N. Koch, Nat. Mater. **7**, 326 (2008).
[25]M. Schwarze, W. Tress, B. Beyer, F. Gao, R. Scholz, C. Poelking, K. Ortstein, A. A. Günther, D. Kasemann, D. Andrienko, and K. Leo, Science **352**, 1446 (2016).
[26]G. Heimel, I. Salzmann, S. Duhm, and N. Koch, Chem. Mater. **23**, 359 (2011).
[27]W. N. Han, K. Yonezawa, R. Makino, K. Kato, A. Hinderhofer, R. Murdey, R. Shiraishi, H. Yoshida, N. Sato, N. Ueno, and S. Kera, Appl. Phys. Lett. **103**, 253301 (2013).
[28]S. Blumstengel, H. Glowatzki, S. Sadofev, N. Koch, S. Kowarik, J. P. Rabe, and F. Henneberger, Phys. Chem. Chem. Phys. **12**, 11642 (2010).
[29]A. A. Virkar, S. Mannsfeld, Z. Bao, and N. Stingelin, Adv. Mater. **22**, 3857 (2010).
[30]E. Zojer, T. C. Taucher, and O. T. Hofmann, Adv. Mater. Interfaces **6**, 1900581 (2019).
[31]L. Romaner, G. Heimel, C. Ambrosch-Draxl, and E. Zojer, Adv. Funct. Mater. **18**, 3999 (2008).
[32]A. Vilan and D. Cahen, Chem. Rev. **117**, 4624 (2017).
[33]S. P. Pujari, L. Scheres, A. T. M. Marcelis, and H. Zuilhof, Angew. Chem. Int. Ed. **53**, 6322 (2014).
[34]E. L. Hanson, J. Guo, N. Koch, J. Schwartz, and S. L. Bernasek, J. Am. Chem. Soc. **127**, 10058 (2005).
[35]P. J. Hotchkiss, S. C. Jones, S. A. Paniagua, A. Sharma, B. Kippelen, N. R. Armstrong, and S. R. Marder, Acc. Chem. Res. **45**, 337 (2012).
[36]M. Timpel, M. V. Nardi, S. Krause, G. Ligorio, C. Christodoulou, L. Pasquali, A. Giglia, J. Frisch, B. Wegner, P. Moras, and N. Koch, Chem. Mater. **26**, 5042 (2014).
[37]E. L. Hanson, J. Schwartz, B. Nickel, N. Koch, and M. F. Danisman, J. Am. Chem. Soc. **125**, 16074 (2003).
[38]I. Lange, S. Reiter, M. Pätzel, A. Zykov, A. Nefedov, J. Hildebrandt, S. Hecht, S. Kowarik, C. Wöll, G. Heimel, and D. Neher, Adv. Funct. Mater. **24**, 7014 (2014).
[39]F. Piersimoni, R. Schlesinger, J. Benduhn, D. Spoltore, S. Reiter, I. Lange, N. Koch, K. Vandewal, and D. Neher, J. Phys. Chem. Lett. **6**, 500 (2015).
[40]P. Strobel, M. Riedel, J. Ristein, and L. Ley, Nature **430**, 439 (2004).
[41]N. Koch, S. Duhm, J. P. Rabe, A. Vollmer, and R. L. Johnson, Phys. Rev. Lett. **95**, 237601 (2005).
[42]W. Chen, S. Chen, C. Q. Dong, Y. G. Xing, and A. T. S. Wee, J. Am. Chem. Soc. **129**, 10418 (2007).
[43]T. Schultz, J. Niederhausen, R. Schlesinger, S. Sadofev, and N. Koch, J. Appl. Phys. **123**, 245501 (2018).
[44]Y. Xu, O. T. Hofmann, R. Schlesinger, S. Winkler, J. Frisch, J. Niederhausen, A. Vollmer, S. Blumstengel, F. Henneberger, N. Koch, P. Rinke, and M. Scheffler, Phys. Rev. Lett. **111**, 226802 (2013).
[45]R. Schlesinger, Y. Xu, O. T. Hofmann, S. Winkler, J. Frisch, J. Niederhausen, A. Vollmer, S. Blumstengel, F. Henneberger, P. Rinke, M. Scheffler, and N. Koch, Phys. Rev. B **87**, 155311 (2013).
[46]L. Schöttner, S. Erker, R. Schlesinger, N. Koch, A. Nefedov, O. T. Hofmann, and C. Wöll, J. Phys. Chem. C **124**, 4511 (2020).
[47]R. Schlesinger, F. Bianchi, S. Blumstengel, C. Christodoulou, R. Ovsyannikov, B. Kobin, K. Moudgil, S. Barlow, S. Hecht, S. R. Marder, F. Henneberger, and N. Koch, Nat. Commun. **6**, 6754 (2015).
[48]K. Akaike, M. V. Nardi, M. Oehzelt, J. Frisch, A. Opitz, C. Christodoulou, G. Ligorio, P. Beyer, M. Timpel, I. Pis, F. Bondino, K. Moudgil, S. Barlow, S. R. Marder, and N. Koch, Adv. Funct. Mater. **26**, 2493 (2016).
[49]T. Schultz, D. Lungwitz, E. Longhi, S. Barlow, S. R. Marder, and N. Koch, Adv. Funct. Mater. **31**, 2010174 (2021).
[50]M. H. Futscher, T. Schultz, J. Frisch, M. Ralaiarisoa, E. Metwalli, M. V. Nardi, P. Müller-Buschbaum, and N. Koch, J. Phys.: Condens. Matter **31**, 064002 (2019).
[51]R. Wang, Y. Wang, C. Wu, T. Zhai, J. Yang, B. Sun, S. Duhm, and N. Koch, Adv. Funct. Mater. **30**, 1903440 (2020).
[52]Z. Wang, P. Li, Z. Liu, J. Fan, X. Qian, J. He, S. Peng, D. He, M. Li, and P. Gao, APL Mater. **7**, 110701 (2019).
[53]W. Fang, P. Wang, Z. Ni, T. Sun, C. Xiang, K. Yue, R. Wang, J. Yang, Y. Zhou, C. Wang, and Y. Yang, Adv. Mater. Interfaces **7**, 2000754 (2020).
[54]L.-M. Yu, T. Chen, N. Feng, R. Wang, T. Sun, Y. Zhou, H. Wang, Y. Yang, and Z.-H. Lu, Sol. RRL **4**, 1900513 (2020).
[55]V. H. Nguyen, S. Kato, K. Gotoh, Y. Kurokawa, and N. Usami, Sustainable Energy Fuels **3**, 1448 (2019).
[56]M.-U. Halbich, D. Zielke, R. Gogolin, R. Sauer-Stieglitz, W. Lövenich, and J. Schmidt, Sci. Rep. **9**, 9775 (2019).
[57]D. Cohen, E. Thakur, and M. G. Walter, Pure Appl. Chem. **93**, 1109 (2021).
[58]Y. Zhou, C. Fuentes-Hernandez, J. Shim, J. Meyer, A. J. Giordano, H. Li, P. Winget, T. Papadopoulos, H. Cheun, J. Kim, M. Fenoll, A. Dindar, W. Haske, E. Najafabadi, T. M. Khan, H. Sojoudi, S. Barlow, S. Graham, J. L. Brédas, S. R. Marder, A. Kahn, and B. Kippelen, Science **336**, 327 (2012).
[59]E. Orgiu, N. Crivillers, M. Herder, L. Grubert, M. Pätzel, J. Frisch, E. Pavlica, D. T. Duong, G. Bratina, A. Salleo, N. Koch, S. Hecht, and P. Samorì, Nat. Chem. **4**, 675 (2012).
[60]T. Mosciatti, M. G. del Rosso, M. Herder, J. Frisch, N. Koch, S. Hecht, E. Orgiu, and P. Samorì, Adv. Mater. **28**, 6606 (2016).
[61]Z. Zhang, X. Liu, Z. Li, Z. Chen, F. Zhao, F. Zhang, and C. H. Tung, Adv. Funct. Mater. **18**, 302 (2008).
[62]R. C. Shallcross, P. Zacharias, A. Köhnen, P. O. Körner, E. Maibach, and K. Meerholz, Adv. Mater. **25**, 469 (2013).
[63]G. Ligorio, G. F. Cotella, A. Bonasera, N. Zorn Morales, G. Carnicella, B. Kobin, Q. Wang, N. Koch, S. Hecht, E. J. W. List-Kratochvil, and F. Cacialli, Nanoscale **12**, 5444 (2020).
[64]Q. Wang, G. Ligorio, V. Diez-Cabanes, D. Cornil, B. Kobin, J. Hildebrandt, M. V. Nardi, M. Timpel, S. Hecht, J. Cornil, E. J. W. List-Kratochvil, and N. Koch, Adv. Funct. Mater. **28**, 1800716 (2018).